

Gradient Sensing via Cell Communication

Dallas Foster · Collin Victor · Brian
Frost · Juan M. Restrepo

Received: date / Accepted: date

Abstract The chemotactic dynamics of cells and organisms that have no specialized gradient sensing organelles is not well understood. In fact, chemotaxis of this sort of organism is especially challenging to explain when the external chemical gradient is so small as to make variations of concentrations minute over the length of each of the organisms. Experimental evidence lends support to the conjecture that chemotactic behavior of chains of cells can be achieved via cell-to-cell communication. This is the chemotactic basis for the Local Excitation, Global Inhibition (LEGI) model.

A generalization of the model for the communication component of the LEGI model is proposed. Doing so permits us to study in detail how gradient sensing changes as a function of the structure of the communication term. The key findings of this study are, an accounting of how gradient sensing is affected by the competition of communication and diffusive processes; the determination of the scale dependence of the model outcomes; the sensitivity of communication to parameters in the model. Together with an essential analysis of the dynamics of the model, these findings can prove useful in suggesting experiments aimed at determining the viability of a communication mechanism in chemotactic dynamics of chains and networks of cells exposed to a chemical concentration gradient.

Keywords chemotaxis, chemical gradient, cell signaling, LEGI

D. Foster
Department of Mathematics, Oregon State University, Corvallis OR 97331,

C. Victor
Mathematics Department, University of Nebraska at Lincoln, Lincoln NE 68588,

B. Frost-LaPlante
Electrical Engineering, Cooper Union, New York NY 10003,

J.M. Restrepo
Department of Mathematics, Oregon State University, Corvallis OR 97331 and Kavli Institute of Theoretical Physics, University of California Santa Barbara, Santa Barbara, CA 93106

1 Introduction

Chemotaxis refers to the movement, and by extension to the organization, of cells and organisms that react to chemical stimulus. Some chemotactic organisms have identifiable structures which are thought to allow these to sense a chemical gradient. However, plenty of chemotactic cells and organisms do not have clearly-defined chemical receptors that enable these to distinguish a bias in the chemical gradient. Chemotaxis for these organisms is even more difficult to understand when they are small compared to the distance required to sense a gradient by some electrochemical means in noisy environments. For freely moving organisms there are a number of models based upon clustering due to collisional or screening effects owing to the combined effect of diffusive and drift processes ([2]). For cells, such as those involved in certain healing processes and prenatal development, where cells are in contact but have topological development biases that are thought to be, to some extent, chemically enabled, an alternative chemotactic mechanism is thought to play a role, namely, chemotaxis mediated by intercellular communication. In this scenario the gradient sensing in the microorganism involves resolving the differential chemical concentration, as compared with a background concentration. The background concentration is determined by a consensus of concentration levels in neighboring cells in the chain [1].

The Local Excitation, Global Inhibition (LEGI) model, initially proposed in [3], captures gradient detection via inter-cellular communication. Fundamental to the model is whether cells can discern differences between the local chemical concentration and a background concentration, in the presence of noise. Experimental evidence for the sensitivity of gradient detection of cell cohesion and spatial scale demonstrate reduced signal noise chemical concentration differentiation with cell chain size (see [4]). The LEGI formalism, as implemented in [5], captures cell communication via nearest neighbor exchanges of chemical concentrations. Further laboratory experiments have tested critical aspects of the chemotactic mechanism in the LEGI formalism (See [7]).

The model captures the interplay of diffusive processes, noisy reactions, and intercellular communication of a cell chain exposed to an external chemical gradient. An analysis would go a long way in determining how these 3 effects play out, particularly as the system evolves in time. In what follows we undertake such analysis, taking the opportunity to modify the LEGI as described in [5] by generalizing the communication mechanism. It is hoped that doing so will suggest laboratory experiments that can further constrain the model and determine its validity in explaining chemotaxis among chains of cells as well as how the communication mechanism would play out in different cell species.

Experimental studies have focused on the critical question of cell gradient detection by a comparison to a cell chain reference concentration. The goals of this study are complementary to the laboratory effort. These are, (1) to perform an analysis of the generalized LEGI system with an aim of discerning how the interplay of communication and diffusion play out, as a function of

cell chain length and cell size; (2) to explore how several straightforward approximations of the communication mechanism affect chemotactic outcomes. It is hoped that the insights in this exercise will be helpful in interpreting laboratory observations; (3) to discern how system size plays a role in determining gradient sensing. In this scenario the signal-to-noise ratio of the live system is critical. (In the LEGI model thermal noise enters in a very straightforward way and thus is not highlighted here, nevertheless full consideration of this issue is outside of the scope of this study); (4) to explain how the competition of communication and diffusive processes play out in time; (5) to quantify the effective correlation length of communication as a function of cell size and model for communication; (6) to determine the sensitivity of the outcomes on model parameters critical to the communication mechanism.

2 The LEGI Model

The LEGI is an evolutionary model that captures the reaction equations of a one-dimensional chain of cells, exposed to a diffusing external chemical concentration (see [5]). Its distinguishing feature is the presence of cell-to-cell chemical concentration communication. Each cell sports active receptors, r , which interact with the external concentration c . The amount of active local chemical within the cell is denoted by x and y denotes the amount of chemical with intercellular reach. The concentration r for each cell is dependent on the concentration, c around that cell. The activation rates for x and y are assumed to be constant, and denoted by β . The key distinction between x and y is that x is local to each cell whilst y can be passed between cells, at a constant rate γ . Hence x and y are activated and deactivated at the same rate, but the exchange of y between cells leads to differences in amounts of x and y . This difference between the local and global concentrations is proposed to be the underlying signal the cell uses to infer the chemical gradient.

2.1 The Standard LEGI Model

We consider a chain of m cells, each cell of length \tilde{a} . The total length of the cell chain is given by $L = m\tilde{a}$. We denote by c_0 the average value of the dimensional concentration \tilde{c} . Nondimensionalized, the LEGI model is

$$\begin{aligned}
 \frac{\partial c}{\partial t} &= \nabla^2 c - \sum_{n=1}^m \delta\left(\frac{z}{L} - \frac{z_n}{L}\right) \frac{dr_n}{dt}, \\
 dr &= \alpha c_n dt - \mu r_n dt + d\eta_n, \\
 dx &= \beta r_n dt - \nu x_n dt + d\xi_n, \\
 dy &= \beta r_n dt + \sum_{n'=1}^m M_{nn'} y_{n'} dt + d\chi_n, \\
 M &= \delta_{n,n'}(-\nu - 2\gamma) + (\delta_{n-1,n'} + \delta_{n+1,n'})\gamma,
 \end{aligned} \tag{1}$$

where the position is $z = \tilde{z}/L$, and time is $t = \tilde{t}D/L^2$. The n^{th} cell is located at z_n . The non-dimensionalized rates $\alpha, \beta, \mu, \nu, \gamma$ are obtained by multiplying their dimensional counterparts by \tilde{a}^2/D . Similarly, each chemical concentration is inversely scaled by c_0 . From this point on when we refer to $a = \tilde{a}/L = 1/m$ as the non-dimensional cell size. Equation (1) is a system of coupled differential equations where the modified diffusion equation for c is coupled with a total of $3m$ equations for r, x , and y . M is a symmetric, nearest-neighbor coupling term. Thermal fluctuations are captured by $d\eta, d\xi$, and $d\chi$, representing uncorrelated incremental Wiener processes with known variances.

The scaled LEGI model can be written more compactly as follows: Let $\mathbf{v}(t)$ and $d\mathbf{W}$ be vectors of length $3m$ defined, respectively, by

$$\mathbf{v}(t) = \begin{pmatrix} \mathbf{r}(t) \\ \mathbf{x}(t) \\ \mathbf{y}(t) \end{pmatrix}, \quad d\mathbf{W} = \begin{pmatrix} d\eta \\ d\xi \\ d\chi \end{pmatrix}.$$

Let A, B , and C be the rate matrices

$$A = -\mu I_m, \quad B = \beta I_m, \quad C = -\nu I_m, \quad (2)$$

where I_m is the $m \times m$ identity matrix. The system (1) can thus be recast as

$$\begin{aligned} \frac{\partial c}{\partial t} &= \nabla^2 c - \sum_{n=1}^m \delta\left(\frac{z}{L} - \frac{z_n}{L}\right) \frac{dr_n}{dt}, \\ d\mathbf{v} &= R\mathbf{v}dt + \mathbf{F}dt + d\mathbf{W} \end{aligned} \quad (3)$$

where

$$R = \begin{pmatrix} A & 0_m & 0_m \\ B & C & 0_m \\ B & 0_m & M \end{pmatrix}, \quad \mathbf{F} = \begin{pmatrix} \alpha \mathbf{c} \\ \mathbf{0} \\ \mathbf{0} \end{pmatrix}.$$

The 0_m represent $m \times m$ zero matrices and $\mathbf{0}$ the column vector of zeros with length m . In the ensuing analysis we will not have occasion to highlight the role played by the diffusion processes and thus we will omit these further on.

3 Generalization of the LEGI Model

Neglecting stochasticity, the continuous-space version of the model is

$$\begin{aligned}\frac{\partial c}{\partial t} &= \nabla^2 c - \alpha c + \mu r, \\ \frac{\partial r}{\partial t} &= \alpha c - \mu r, \\ \frac{\partial x}{\partial t} &= \beta r - \nu x, \\ \frac{\partial y}{\partial t} &= \beta r - \nu y - \gamma(w * y),\end{aligned}\tag{4}$$

for $t > 0$ and $z \in \Omega$, the physical domain. In the above equations $r(z, t)$, $x(z, t)$, and $y(z, t)$ represent the concentrations, and these are assumed known at $t = 0$. We will refer to the last term in the y equation of (4) as the *communication term*. It is the convolution of y and a weight function w . The (spatial) convolution is defined as

$$(w * y)(z, t) = \int_{-\infty}^{\infty} w(u)y(z - u, t) du.\tag{5}$$

We will dispense with any complications that arise from boundary conditions. The system (4) is thus the continuous-space counterpart to (3), formally, in the large m and small a limit. In some of our later discussions it will be convenient to cast (4), formally, as

$$\frac{dy}{dt} = L^{-1}[\mathcal{A}f(y, c)],\tag{6}$$

where L^{-1} is a complicated linear operator and \mathcal{A} is a spatially-mollifying operator. In (1) we identify this operator with the operator M , and f is a known function relating c and y . Alterations to the convolution term affect the averaging operator \mathcal{A} and one can consider, in the finite dimensional case, $\mathcal{A} = M + \delta M$, where δM is some perturbation of M .

3.1 The Convolution Term

In order to investigate the impact of chemical communication in (4) we focus on the convolution kernel w . Among the properties of relevance to the physics, translational symmetry dictates that the kernel w have the property

$$\int_{\Omega} w(z)dz = 0.$$

Furthermore, w should not endow directional preferences to the fluxes of concentration. Hence, w should be spatially symmetric.

The original LEGI becomes a special case of the general model, under certain approximations and assumptions. Denoting ϵ the distance between cell centers, w is explicitly given by

$$w = 2\delta(z) - \delta(z - \epsilon) - \delta(z + \epsilon), \quad (7)$$

where δ is the dirac distribution. More nonlocal kernels can be proposed and their impact on the LEGI model can be analyzed. For example, a family of continuous kernels that satisfy the physical constraints follow the proposition

$$f_k(z) = (-1)^n \frac{d^{2n}}{dz^{2n}} \left(e^{-z^2/2\sigma} \right), \quad n = 1, 2, 3, \dots \quad (8)$$

where σ is a parameter controlling the effective width of the kernel function. This family extends the spatial range of dependence of the local concentration to encompass more cells, with the physical implication that cell chemical concentrations correlate at shorter or longer distances. The competition of background diffusion processes and intercellular concentration exchanges can manifest themselves differently in time and can be classified by the relative size of the diffusion length scale and the correlation length scale. Furthermore, we can consider how this tension between diffusion and communication plays out when the cells are spatially resolved and better characterized as a chain of discrete neighboring cells.

We analyze first the operator when the support of w is small. Following [6], we expand y into a Taylor series centered at z , obtaining, to lowest order, a second-order operator approximation. To see this,

$$\int_{-\infty}^{\infty} w(u)y(z-u, t) du \approx \int_{-\infty}^{\infty} w(u) \left(y(z, t) - uy'(z, t) + \frac{u^2}{2}y''(z, t) \right) du. \quad (9)$$

Breaking this up into three integrals and taking the u -independent terms out, we get

$$y(z, t) \int_{-\infty}^{\infty} w(u) du - y'(z, t) \int_{-\infty}^{\infty} uw(u) du + y''(z, t) \int_{-\infty}^{\infty} \frac{u^2}{2}w(u) du. \quad (10)$$

By employing the properties that w must satisfy, the first two integrals in the preceding expression are zero. The remaining integral is a number solely dependent on the particular kernel in use. We call this number Ω_1 , allowing us to simply write

$$w * y \approx y''(z, t) \int_{-\infty}^{\infty} \frac{u^2}{2}w(u) du = \Omega_1 y''(z, t). \quad (11)$$

Replacing this approximation into the last equation of (4) we obtain

$$\frac{\partial y}{\partial t} = \beta r(z, t) - \nu y(z, t) + \Omega_1 \gamma y''(z, t). \quad (12)$$

In the case where the diffusion gradient is steep, *i.e.*, the diffusion scale is small compared to the correlation length of communication, the manner in which the kernel is mapped onto a discrete cell chain becomes important. Namely, some approximations lead to sensitive dependence of chemotaxis estimates on the nature of the kernel, and more importantly,

3.2 Cell-Resolved Cases

The original LEGI model is obtained when a second-order finite difference approximation to (12)

$$y''(z, t) = \frac{y(z + a, t) - 2y(z, t) + y(z - a, t)}{a^2} + O(a^2), \quad (13)$$

is used on (12). Where $a = 1/m$ represents the size of each cell in the model. This approximation is effectively dictating that each cell can only communicate with its two adjacent cells per unit of time. The approximation of the Laplacian operator by a second-order finite difference brings in another finite-size question: If the number of cells is large enough and cell size is small enough it might be reasonable to contend that the radius of communication can be larger. Alternatively, we could approximate $y''(z, t)$ by

$$y''(z, t) = \frac{-y(z + 2a, t) + 16y(z + a, t) - 30y(z, t) + 16y(z - a, t) - y(z - 2a, t)}{12a^2} + O(a^4). \quad (14)$$

This second approximation couples 5 cells, rather than 3. As we will show, this has a bearing on the time evolution of the LEGI, as applied to certain discrete chains.

An alternative kernel approximation is obtained by retaining higher order terms in the Taylor expansion (9). The next higher order approximation results in

$$\frac{\partial y}{\partial t} \approx \lambda(\beta r(z, t) - \nu y(z, t) + \Omega_1 \gamma y''(z, t) + \Omega_2 \gamma y^{(4)}(z, t)), \quad (15)$$

where Ω_2 is defined by

$$\Omega_2 = \frac{1}{24} \int_{-\infty}^{\infty} w(u) u^4 du, \quad (16)$$

with a lowest-order finite-cell representation

$$y^{(4)}(z) = \frac{y(z + 2a) - 4y(z + a) + 6y(z) - 4y(z - a) + y(z - 2a)}{a^4} + O(a^2). \quad (17)$$

External concentration gradients in micro-biological systems will typically not exhibit the variability one would expect to make the retention of the fourth derivative term much different from the second derivative, and further, thermal noise in the system might swamp these differences.

3.3 Comparison of Communication Generalizations

We will present a few calculations that describe how some of the model differences in the communication term influence the chemotactic dynamics, particularly when the system size is incorporated in the complexity of the system. We simulate (1) with both second and fourth order finite difference approximation

# of Cells	Method	5 Cells	20 Cells	100 Cells
$c(z, 0) = z$	Original LEGI	0.43118	0.42838	0.428488
	$y^{(2)}$ correction	0.43103	0.42837	0.428488
	$y^{(4)}$ correction	0.43103	0.42837	0.428488
$c(z, 0) = z^4$	Original LEGI	0.53390	0.42402	0.42946
	$y^{(2)}$ correction	0.41638	0.42743	0.42947
	$y^{(4)}$ correction	0.41732	0.42722	0.42947

Table 1 Numerical solutions were run with the given number of cells up to a time $t = 5$. The table contains relative norms measured over space and time with respect to the steady state solution (18). Differences between approximations are largest for nonlinear initial concentration and for small cell counts.

for the second derivative (14) separately, and, in addition, implement (15) with a centered finite difference formula. The goal of the following calculation is to highlight that the size of the cell plays a role when choosing a model for communication. Anticipating the findings, when the cell size is small, compared to the total length of the chain, the results are not very sensitive to the choice of model, in the long time limit. The story is more nuanced in the short time limit, but we consider this case further on.

For this numerical experiment we varied the initial concentration between linear, $c(z, 0) = z$, and nonlinear, $c(z, 0) = z^4$, with number of cells = 5, 20, 100. Values for the parameters are chosen to be physically realistic, $\alpha = \mu = \nu = 1, \beta = 10, \gamma = 100$. Then over the interval $t \in (0, 5)$, we compute the relative errors,

$$\|y^* - y_i\|/\|y^*\|, \quad i = 1, 2, 3$$

where y^* is the steady state solution to (4) for the chemical concentration of y ,

$$y^*(z) = \lim_{t \rightarrow \infty} y(z, t) \quad (18)$$

Here the steady state solution is constant and unaffected by choice of discrete convolution w chosen from (13, 14, 15). y_1 is the solution to (1) computed by second order finite difference second derivative communication, y_2 similarly computed by fourth order finite difference second derivative communication, while y_3 is computed with implementing (14). All of the experiments were performed without noise. By comparing each solution with (18) we can see which solutions reach equilibrium the fastest.

When the initial concentration is linear, the percent difference of the two modified implementations from the original LEGI model solution is less than .1% and decreases as the number of cells increase. In the nonlinear case, there is a noticeable difference of 12% between the LEGI and higher order approximations when the cell sizes are relatively large. As theory predicts, this distinction decreases as the size cell size a becomes very small, i.e. the number of cells -

m - increase and the approximations of (5) become closer to the actual convolution's value. In conclusion, in the long-time limit, the outcomes are sensitive to the manner in which the communication model is formulated.

The short-time limit is more interesting and it emphasizes more directly the competition between diffusive and communication effects. Consider the following idealized experiment: the initial concentrations of c, r are set to zero everywhere, y is initialized as zero in each cell, except the center cell, taken to be $z = 0$, which has an initial value of one. Since c and r are zero everywhere for every time-step, the only manner in which y changes are by deactivation and communication. In the very earliest time-steps, this change is heavily dominated by communication, as γ is typically 10 – 100 times larger than ν . In the early moments, we look to see the properties of communication between cells with respect to both distance and time. Using the same notation for each solution, we look at the autocorrelation, \hat{y}_i , of each y_i in space. This is done by application of the Wiener-Kinchin theorem, which is justified by the finite length of y . That is

$$\hat{y}_i = \mathcal{F}^{-1}(\mathcal{F}(y_i)\overline{\mathcal{F}(y_i)}),$$

where \mathcal{F} is the Fourier transform (defined below). Graphs of \hat{y}_i after 25 time steps ($t = 0.5$) are shown in Figure (1a). The figures convey the differences between the three communication methods at the early times. Larger sample correlation imply longer correlation lengths and further spread of the chemical y . Here we see that the fourth derivative correction clearly increases the rate of communication of y the fastest for very short time scales. These results concur with our estimation that a larger effective communication radius leads to faster flow. Figure (1b) shows the evolution of the wave of information over time, we record how long it takes for the concentration in y in a cell Δn units away from the dirac initial condition to exceed a tolerance of 10^{-4} . For a radius of roughly 18 cells, the fourth derivative correction term spreads the chemical y faster than either the original LEGI model or second derivative correction. This result matches are intuition, but after a certain distance from the origination of the wave, the original LEGI solution reaches the cells faster.

4 The Competition of Diffusion and Communication and Sensitivity Analysis

We turn our attention now to the competition of diffusion and communication and its implications to chemotactic dynamics situation.

4.1 The Time-Steady State

For completeness, we first summarize the steady state. It is clear from (6) that when $\dot{y} = 0$, $f(c)$ lies in the kernel of the averaging (diffusion) operator \mathcal{A} . In

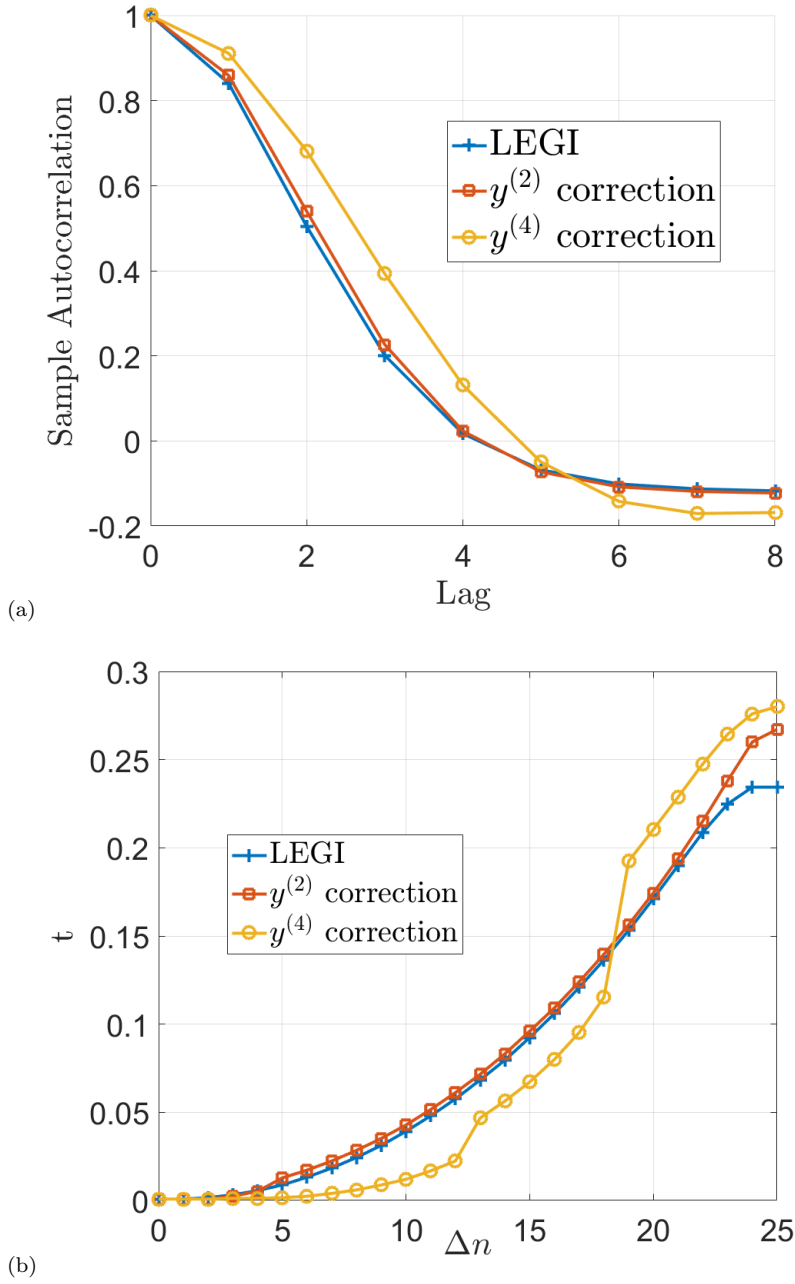


Fig. 1 (a) The sample autocorrelation is computed for the solution generated by implementing each of the three communication terms. Larger autocorrelation suggests enhanced communication. (b) The amount of nondimensionalized time it takes for a cell Δa units away from $\delta(z)$ initial condition to have a value larger than 10^{-4} is given as a proxy for cell communication. In these tests constants were taken to be $\alpha = \mu = \nu$, $\beta/\nu = 10$, $\gamma/\nu = 100$. The parameter values are suggested in [5].

particular, solving (4) yields

$$\begin{aligned}\nabla^2 c &= 0, \\ r &= \frac{\alpha}{\mu} c, \\ x &= \frac{\beta}{\nu} r, \\ y &= \mathcal{F}^{-1} \left\{ \frac{\frac{\beta}{\nu} \hat{r}}{1 + \frac{\gamma}{\nu} \hat{w}} \right\},\end{aligned}$$

where \mathcal{F} is the spatial Fourier transform (defined explicitly below). The amount of c , taken to be either a constant or a linear gradient, yields r . When $\gamma = 0$, we obtain the solution with no communication term and it is, to with a constant, the same as c . When the communication term is non-zero, the ratio of γ to ν as well as the support of the w have a bearing on the magnitude of y (as well as the extent in space affected by communication).

4.2 Transient Dynamics

We examine the role played by deactivation and communication of the chemical y on the dynamics transient dynamics. The key parameters are ν and γ . The analysis is easily performed using Fourier transforms. The system (4) in Fourier space is

$$\begin{aligned}\frac{\partial \hat{c}}{\partial t}(k, t) &= -k^2 \hat{c} - \alpha \hat{c} + \mu \hat{r}, \\ \frac{\partial \hat{r}}{\partial t}(k, t) &= \alpha \hat{c} - \mu \hat{r}, \\ \frac{\partial \hat{x}}{\partial t}(k, t) &= \beta \hat{r} - \nu \hat{x}, \\ \frac{\partial \hat{y}}{\partial t}(k, t) &= \beta \hat{r} - \nu \hat{y} - \gamma \hat{w} \hat{y},\end{aligned}$$

where $\hat{c}, \hat{r}, \hat{x}, \hat{y}, \hat{w}$ denote the Fourier counterparts to the original space variables. Note that $\hat{w}(k)$ is solely a function of the wavenumber k . This system of ordinary differential equations is linear, and we can represent it in matrix form as

$$\frac{\partial}{\partial t} \hat{\mathbf{Y}}(k, t) = \mathcal{A}(k) \hat{\mathbf{Y}}(k, t), \quad t > 0. \quad (19)$$

The solution of this equation is

$$\hat{\mathbf{Y}}(k, t) = e^{\mathcal{A}(k)t} \hat{\mathbf{Y}}(k, 0) = P e^{At} P^{-1} \hat{\mathbf{Y}}(k, 0), \quad t \geq 0, \quad (20)$$

where $\mathcal{A} = PAP^{-1}$ is the diagonalization of $\mathcal{A}(k)$ where the dependence on k has been suppressed. In order to explore outcomes as a function of γ and

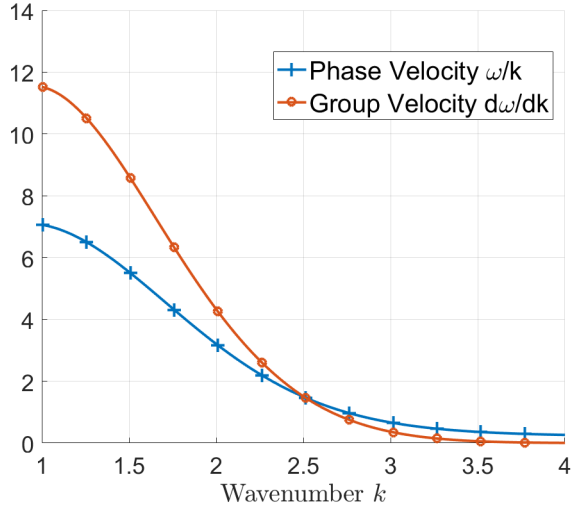


Fig. 2 Comparison of Phase and Group Velocities for $\gamma \approx 10\nu$ for (21). Here, $w(z)$ was chosen from the family (8).

ν , we consider the evolution in time of the system subject to a Dirac delta distribution in y at $t = 0$. In this case,

$$y(z, t) = \frac{1}{\sqrt{2\pi}} \int_{-\infty}^{\infty} \hat{y}(k, 0) e^{ikz} e^{-t(\gamma\hat{w}(k)+\nu)} dk. \quad (21)$$

From this expression, it is easy to see that the dispersion relation for this system of differential equations is given by

$$\omega(k) = i(\gamma\hat{w}(k) + \nu).$$

We note that $\gamma \geq 0$ and $\nu \geq 0$. Further the physically-relevant parameter regime is $\gamma > \nu$, which is to say that the solution is highly dispersive, owing to the communication mechanism. For $\gamma = 10\nu$, Figure 2 depicts the phase and group velocities v_p, v_g respectively, defined as,

$$v_p = \omega(k)/k, \quad \text{and} \quad v_g = \frac{d\omega}{dk}.$$

Notice that $v_p(k)$ is generally unbounded as $k \rightarrow 0$ while $v_g(k)$ is bounded for all k and takes on the value zero at the origin. Furthermore, if we postulate that w decays exponentially, then $v_p > v_g$ for large enough values of k . This intersection is directly related to the support of $w(k)$. Since, dimensionally speaking $k = \tilde{k}L$, then we are only interested in wave numbers where $\tilde{k} > 1/L$ and $k > 1$. It is for these small wave numbers (large wavelengths) that the group velocity, the speed at which information in the system travels, is more significant. Only for smaller wavelengths does the phase velocity marginally

exceed the group velocity. It is this relationship that is relevant when comparing various models for communication. The observation that larger support of the kernel $w(k)$ leads to the group velocity dominating phase velocity over smaller and smaller wave lengths supports this hypothesis. The phase velocity weights the deactivation constant ν greater relative to the communication parameter γ for small wavenumber and the diffusion contributions from \hat{w} , indicating that for these waves deactivation influences their individual velocities to a greater extent. The group velocity, meanwhile, does not incorporate ν and therefore indicates that wave packets are driven more by communication.

The dispersion relation and group velocity for the LEGI model solution, second derivative correction, and fourth derivative correction are shown in Figures 3a and 3b, respectively. Both the dispersion relation and group velocities are sinusoids, with roughly only the first period shown. The relationship between the phase and group velocity for each of the approximations parallel Figure 1. Here we rely on the interpretation of the group velocity as the speed at which information travels through the system. The fact that the fourth derivative correction term exhibits a larger group (and phase) velocity indicates that it should propagate information faster through the system (at least at large wavelengths). The conclusion from Figure 3 is to reinforce the notion that higher order operators induces larger wave velocities and therefore leads to greater speed of communication.

Assuming $\hat{w}(k)$ is sufficiently smooth, we can represent it in terms of a Taylor expansion about a particular point, which we truncate at the quadratic term. Keeping with our original assumptions about w (important here is that w is even) then we can simplify this series and write the solution as

$$y(z, t) = \frac{e^{-t(\gamma\hat{w}_0+\nu)}}{2\pi} \int e^{-i(kz-i\gamma k^2/2\hat{w}_0''t)} dk. \quad (22)$$

We are able to calculate this Fourier Transform analytically, giving us the approximate solution for $y(z, t)$,

$$y(z, t) = \frac{e^{-t(\gamma\hat{w}_0+\nu)-\frac{z^2}{2\hat{w}_0''\gamma t}}}{\sqrt{2\pi\hat{w}_0''\gamma t}}. \quad (23)$$

Having this expression enables a fruitful analysis of the chemical's dependence on the parameters ν, γ .

There are three immediate conclusions that can be drawn from this formula. First, for a fixed t , γ acts as to control the width of the pseudo-Gaussian distribution that y has. This matches the intuition and physical reasoning that γ , being the communication parameter, diffuses the chemical y among the cells in the system. Similarly, ν acts only in as a rate of exponential decay. This again intuitively matches are expectation that ν controls the rate of deactivation of y . Furthermore, the entire expression $\gamma\hat{w}_0 + \nu$ is responsible for exponential decay. Lastly, when t is relatively small, the importance of γ is greater than ν . For larger values of t , the decay term is larger than than the

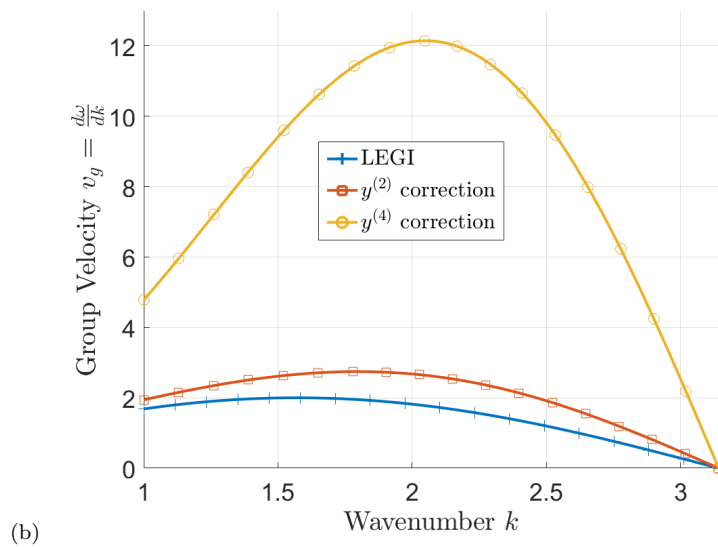
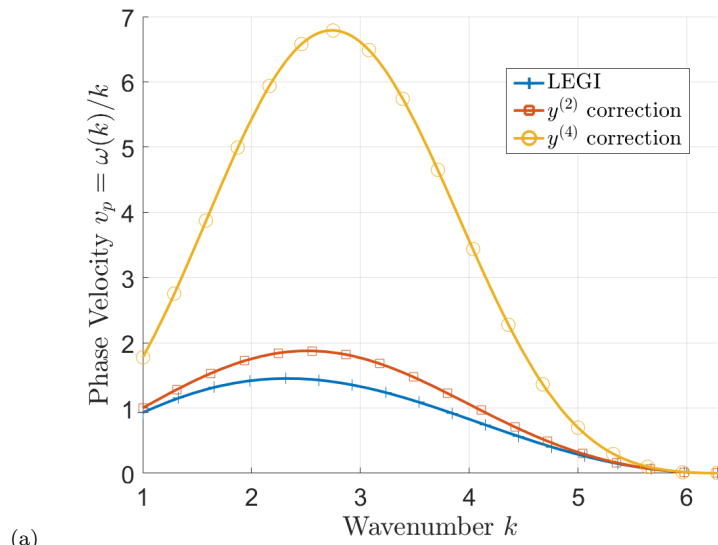


Fig. 3 (a) Dispersion relation corresponding to three approximations for the convolution term in (4). The LEGI model uses (13), (14) uses a modified second derivative approximation, and finally (15) includes the fourth derivative term to the approximation of (4). (b) Similarly, the group velocities for these three approximations.

diffusive term and the relative importance of γ and ν hinges on the value of \hat{w}_0 .

4.3 Sensitivity to Parameters

We investigate the sensitivity (in forward-time) of the LEGI system to changes in the parameter vector $p = [\gamma, \nu]^\top$ (the $(\cdot)^\top$ indicates transpose). These estimates may prove useful in the interpretation and comparisons of model and experimental results.

Since the system is linear, the sensitivity analysis that follows should be robust and comprehensive. We solve the following system of differential equations

$$\frac{\partial}{\partial t} \left(\frac{\partial \hat{Y}}{\partial p_j} \right) = \mathcal{A}(k) \frac{\partial \hat{Y}}{\partial p_j} + \frac{\partial(\mathcal{A}\hat{Y})}{\partial p_j}, \quad \text{for } j = 1, 2. \quad (24)$$

The resulting solutions will give us spatio-temporal information about the relative sensitivity of our system to changes in the values of γ and ν . With this information we can create heuristic regimes in which the system operates. The solution of (24) is given by

$$\frac{\partial \hat{Y}}{\partial p_j}(k, t) = e^{\mathcal{A}(k)t} \frac{\partial \hat{Y}}{\partial p_j}(k, 0) + \int_0^t e^{(t-s)\mathcal{A}(k)} \frac{\partial(\mathcal{A}\hat{Y}(k, s))}{\partial p_j} ds. \quad (25)$$

In particular, continuing with the particular scenario that we have analyzed heretofore,

$$\frac{\partial \hat{y}}{\partial p}(k, t) = -\frac{e^{-t(\nu+\gamma\hat{w})}}{\sqrt{2\pi}} [\hat{w}, 1]^\top = -\hat{y}(k, t)[[\hat{w}, 1]^\top]. \quad (26)$$

We find that the ratio of these sensitivities is exactly the kernel \hat{w} , and therefore the relative importance (the ratio) of these two parameters is constant in time and is captured 'in space' by the structure of \hat{w} . With regard to the kernel generating function (8), the key parameter is σ , which controls the variance of each function. Here, increasing σ , *i.e.*, the correlation length of communication, corresponds to an increasing sensitivity to the parameter γ . This outcome has a bearing on signal-to-noise studies, such as those pursued experimentally in [5].

If we take the inverse Fourier transform of (26), we find that

$$\frac{\partial y(z, t)}{\partial p} = -[(w * y)(z, t), y(z, t)]^\top. \quad (27)$$

Increasing the number of cells which can communicate increases the system's sensitivity to changes in the communication parameter relative to the deactivation parameter. Finally, in another light, the spatial regimes in which the system is more sensitive to communication or deactivation the other is defined by where $w(z) = 1$.

5 Discussion and Concluding Remarks

A generalization is proposed of a model that describes cellular chemotaxis via the competition of thermal effects, reaction-diffusion, and intercellular communication. The model being generalized is known as Local Excitation Global Inhibition (LEGI) and it was proposed by Levchenko and collaborators, [3]. The generalized LEGI model is analyzed with the aim of establishing how cell size, cell chain length, and alternative proposals for the intercell communication manifest themselves in the chemotactic model outcomes. We also determined regimes in space and time where one is expected to see diffusion-dominated or advective-dominated (via communication) reactions. Additionally, sensitivity of the outcomes of the model with regard to parameters were derived. These last two estimates, we argue, could prove useful in interpreting existing experimental results, suggesting new experiments, and comparing the laboratory data to model outcomes and our understanding of cellular chemotaxis.

Although chemotaxis in the LEGI model is made possible by intercell communication, there is no a-priori way, at present, to constrain some of the details in the intercell communication term in the model. This gave us the impetus to consider a general communication model, based upon a convolution operator. This convolution is taken with respect to a generic kernel. The kernel encodes correlations among neighboring cells. The kernel is proposed in continuous space, corresponding to the limit of infinitely small cell size and infinitely large number of cells, for a given total cell chain length. When the correlation length is small, *i.e.* when the effective spatial support of the kernel is small, compared to the length of the chain the chemical concentration is affected by a finite speed signal, propagating through the chain, as well as by diffusion. When we focused on long-time dynamics we determined to what extent the form of the communication model affected the chemotactic process: in the small-cell limit the results were negligibly dependent on the manner in which communication is modeled. In practical terms it is shown that in the small-cell limit comparisons of the LEGI model and laboratory outcomes would be less dependent on the specifics of the communication term, if this term is to be modeled by a convolution.

As would be expected, large gradients were shown to lead to different outcomes with the choice of convolution approximation. In a simple chain of homogeneous cells, we confirmed that unless the system size is not too small, the choice of communication model does not affect significantly the model outcomes. However, it is differences in intercellular concentrations, rather than the external gradient that counts and thus the choice of communication model will be more critical in heterogenous in spatial dimensions higher than one.

In the short time limit one can appreciate and discern how communication and diffusion interplay and how the model results depend on the particular communication proposed. Generally, chemotactic behavior is dominated by the communication term, for short times. This presumably has consequences in some settings when the chemical gradient changes over time. With regard to the communication model it is found that longer correlation lengths lead to

faster signal times. It thus might prove useful, if at all possible experimentally, to determine the speed and dispersion of chemical transport in a cell chain, when subjected to a transient change in the gradient. This would lead to a better model as well as better understanding of the chemotactic mechanism in practical cases.

The effect of thermal noise was ignored in this study. The model is linear and thus changes in isotropic thermal effects will manifest themselves in the variance and covariance fields. These fields were not discussed in this study. Two obvious lines of inquiry, for a future study, are consideration of non-isotropic diffusion, which can introduce extra time and length scales, as well as consideration of chemotaxis in multiple dimensions.

Acknowledgements

JMR wishes to thank the Kavli Institute of Theoretical Physics (KITP), at the University of California, Santa Barbara for their hospitality and for supporting his research on this project. The KITP is supported in part by the National Science Foundation under Grant No. NSF PHY-1748958. CV and BF were Research Experiences for Undergraduate participants at Oregon State University in summer of 2017. The REU program is sponsored by the National Science Foundation. The authors wish to thank Prof. Andrew Mugler and Prof. Bo Sun for helpful discussions.

References

1. Ellison, D., Mugler, A., Brennan, M., Lee, S., Huebner, R., Shamir, E.: Cell-cell communication enhances the capacity of cell ensembles to sense shallow gradients during morphogenesis. *Proc Natl Acad Sci U S A* **113**(6), 679–688 (2016)
2. Keller, E., Segel, L.: Initiation of slime mold aggregation viewed as an instability. *J. theor. Biol.* **26**, 399–415 (1970)
3. Levchenko, A., Iglesias, P.: Models of eukaryotic gradient sensing: Application to chemotaxis of amoebae and neutrophils. *Biophysical Journal* **82**, 50–63 (2002)
4. Malet-Engra, G., Yu, W., Oldani, A., J, R.B., Gov, N., Scita, G., Dupre, L.: Collective cell motility promotes chemotactic prowess and resistance to chemorepulsion. *Curr Biol* **25**(2), 445–457 (2015)
5. Mugler, A., Levchenko, A., Nemenman, I.: Limits to the precision of gradient sensing with spatial communication and temporal integration. *PNAS* pp. 689–695 (2016)
6. Murray, J.: *Mathematical Biology*, 2 edn. Springer-Verlag Berlin Heidelberg
7. Potter, G., Byrd, T., Mugler, A., Sun, B.: Communication shapes sensory response in multicellular networks. *Proc Natl Acad Sci U S A* **113**(37), 10334–10339 (2016)